ISSN 1674-1056
http://cpb.iphy.ac.cn
http://iopscience.iop.org/cpb
中国物理 B
Chinese Physics
中国物理
Chinese Physics B

Ion population fraction calculations using improved screened hydrogenic model with *l*-splitting

Amjad Ali, G Shabbir Naz, Rukhsana Kouser, Ghazala Tasneem, M Saleem Shahzad, Aman-ur-Rehman, M H Nasim

Citation: Chin. Phys. B . 2018, 27(10): 105201. **doi:** 10.1088/1674-1056/27/10/105201

Journal homepage: http://cpb.iphy.ac.cn; http://iopscience.iop.org/cpb

What follows is a list of articles you may be interested in

Tungsten ion source under double-pulse laser ablation system

Ahmed Asaad I Khalil, Ashraf I Hafez, Mahmoud E Elgohary, Mohamed A Morsy
Chin. Phys. B . 2017, 26(9): 095201. **doi:** 10.1088/1674-1056/26/9/095201

Radiative properties of matter based on quantum statistical method

Rukhsana Kouser, G Tasneem, Muhammad Saleem Shahzad, S Sardar, Amjad Ali, M H Nasim, M Salahuddin
Chin. Phys. B . 2017, 26(7): 075201. **doi:** 10.1088/1674-1056/26/7/075201

Absorption of ultrashort intense lasers in laser-solid interactions

Sheng Zheng-Ming, Weng Su-Ming, Yu Lu-Le, Wang Wei-Min, Cui Yun-Qian, Chen Min, Zhang Jie
Chin. Phys. B . 2015, 24(1): 015201. **doi:** 10.1088/1674-1056/24/1/015201

A thin radar-infrared stealth-compatible structure：Design, fabrication, and characterization

Tian Hao, Liu Hai-Tao, Cheng Hai-Feng
Chin. Phys. B . 2014, 23(2): 025201. **doi:** 10.1088/1674-1056/23/2/025201

Design and realization of magnetic-type absorber with broadened operating frequency band

Zhou Yong-Jiang, Pang Yong-Qiang, Cheng Hai-Feng
Chin. Phys. B . 2013, 22(1): 015201. **doi:** 10.1088/1674-1056/22/1/015201

Ion population fraction calculations using improved screened hydrogenic model with l-splitting

Amjad Ali[1,†], G Shabbir Naz[1], Rukhsana Kouser[1], Ghazala Tasneem[1], M Saleem Shahzad[1], Aman-ur-Rehman[2], and M H Nasim[1]

[1] *Department of Physics and Applied Mathematics, Pakistan Institute of Engineering, and Applied Sciences, Islamabad* 45650, *Pakistan*

[2] *Department of Nuclear Engineering, Pakistan Institute of Engineering, and Applied Sciences, Islamabad* 45650, *Pakistan*

(Received 2 May 2018; revised manuscript received 14 June 2018; published online 27 September 2018)

Ion population fraction (IPF) calculations are very important to understand the radiative spectrum emitted from the hot dense matter. IPF calculations require detailed knowledge of all the ions and correlation interactions between the electrons of an ion which are present in a plasma environment. The average atom models, e.g., screened hydrogenic model with l-splitting (SHML), now have the capabilities for such calculations and are becoming more popular for in line plasma calculations. In our previous work [Ali A, Shabbir Naz G, Shahzad M S, Kouser R, Rehman A and Nasim M H 2018 *High Energy Density Phys.* **26** 48], we have improved the continuum lowering model and included the exchange and correlation effects in SHML. This study presents the calculation of IPF using classical theory of fluctuation for our improved screened hydrogenic model with l-splitting (I-SHML) under local thermodynamic equilibrium conditions for iron and aluminum plasma over a wide range of densities and temperatures. We have compared our results with other models and have found a very good agreement among them.

Keywords: self-consistent average atom model, average ionization state, ion population

PACS: 52.25.Os, 32.30.–r, 31.15.xr **DOI:** 10.1088/1674-1056/27/10/105201

1. Introduction

The simultaneous presence of multi-charge ions in hot and dense plasmas predicted by radiative spectra in different experiments is of critical importance.[1] This is closely relevant to the astrophysical plasma, the plasma found in giant planets like Jupiter, and the plasma created in the inertial confinement fusion (ICF) experiments.[2,3] The calculations of ion population fractions (IPF) are very important for many thermodynamic and radiative properties of such hot dense plasmas. These calculations start with the construction of grand partition function (GPF) for interacting electrons in hot and dense plasma. The GPF contains all the information of how different ions have their energy partitioned among themselves in hot dense plasma. The simplest form of GPF is its construction for Fermi gas, where the particles are not interacting among themselves, and then GPF is developed for hot dense plasma for interacting electrons. Now this GPF contains information of the level population, level charges, and level energies of interacting electrons. Finding the solution of this GPF (to make it factorizable) for the interaction electrons (the case of hot and dense plasma) over all possible configurations is not a trivial task as that can be done in the case of non-interaction electrons. In the latter case, a close form of the generating function can be obtained or we can easily factorize the GPF. However, for the interacting electrons systems, the number of terms in GPF increases rapidly and we have to define some cut-offs on the electron population to get reasonable results. Thus it would be difficult to factorize GPF due to the presence of cross-interaction terms for different electrons of a configuration and due to the conservation of the number of electrons for each charge state in a consistent manner. For this purpose, a detailed atomic code would be needed that include all relevant atomic physics processes for the calculation of electron populations for different ions. These models are broadly divided into detailed level (DL) models[4,5] and average atom (AA) models.[6–8] Another class of models uses a parametric potential method to generate speedy atomic data as implemented in Los Alamos National Laboratory code OPAL.[9] There is a new development on the theoretical basis at Los Alamos implemented in code ChemEOS,[10] which is based on a chemical picture representation for a plasma of interacting ions, atoms, and electrons. This code uses the free-energy-minimization technique for Helmholtz free energy of the interacting species to get thermodynamic functions for the equation of state (EOS) and IPF for the opacity calculation in the ATOMIC code.[11]

The average atom models are becoming more popular for hot and dense plasma studies. This is due to the fact that these models can be used for in-line calculations of the equation of state and opacity data contrary to the detailed leveled atomic calculations. Different versions of AA are proposed in the literature depending upon the form and model of the potential used in calculations and boundary conditions imposed on it. All these models have some limitations and approximations

†Corresponding author. E-mail: amjadali_11@pieas.edu.pk

© 2018 Chinese Physical Society and IOP Publishing Ltd

based on accuracy and speed. These versions of AA models are used in different standard codes, e.g., Thomas Fermi model (TF), quantum statistical model (QSM), or quantum self consistent field (QSCF) as referred in Ref. [12] are used in codes THERMOS, CASSANDRA,[13] OPAQS,[14] etc. Another famous class of AA models is based on the finite temperature density functional theory (FTDFT) which is basically an electron density variational model[15,16] based on Khon–Sham equations developed in codes like multi average ion model (Multi-AIM),[17] while AA model based on screening constants, i.e., screened hydrogenic model with l-splitting (SHML)[18,19] for the construction of hydrogenic potential is used in codes like ATMED,[20] SCAALP,[21] etc.

These models represent an average electron population for a given temperature and density and do not include different ionization stages, therefore, they cannot be used to study the experimental spectroscopic data. Using AA models for such studies started with Green,[22] who calculated the correlation energy and population levels for interacting electrons for using an average atom prescription under local thermodynamic equilibrium (LTE) conditions, and the complex operators was used to form GPF for such system. Another attempt was made by Perrot,[23] who calculated the correlation energy by minimizing the Helmholtz free energy using density functional theory (DFT) for the AA model. He has included the bound–bound, bound–free and free–free electron interaction contributions to the calculation of IPF. Wilson[24] introduced the saddle point technique for correlation energy calculations. In this method, GPF summation is transformed into multidimensional integrals from which it is easier to get IPF. This work was extended by Faussurier[25,26] by proposing classical theory of fluctuations in saddle point technique for the calculation of IPF.

Faussurier[25,26] proposed his version of screened hydrogenic model with l-splitting for the in-line calculation of EOS and opacity for high energy density system, and included IPF calculation by improving the saddle point technique. We have improved this SHML model, I-SHML,[27] regarding continuum lowering potential calculations, and by including the exchange and correlation effects to study the density effect in high energy density systems. We have also developed a computer code named OPASH by implementing this improved version of SHML and presented the results for average charge state calculations for different plasma conditions. In this study, we have included IPF calculation using improved SHML and compared our results with Faussurier model and other models. In the next section, we will briefly describe the I-SHML model and inclusion of IPF calculation will be discussed in Section 3. Results and discussion will be presented in Section 4. In Section 5, we will summarize and conclude our results.

2. Brief introduction of I-SHML

We briefly describe the basic ingredients of SHML[18,19] model and the improvements made by us to lay down some mathematical notation for the next section. SHML is basically an AA model based on the central field approximation in which each electron of a level k ($k = 1 + l_k + n_k(n_k - 1)/2$, where n_k is the principal quantum number and l_k is the angular momentum quantum number) moves in an independent effective hydrogenic potential characterized by Z_k/r, where Z_k is the level screened charge with limitation of $1 \le k \le k_{\max}$. $k_{\max}$ is the maximum number of orbitals considered in the calculation, which in our case is 55 corresponding to all levels up to $n = 10$. In AA the electrons in different levels are not statistically correlated and can be characterized by a fixed number of states, each with a fixed electron occupation number (not necessarily an integer), i.e., a fixed electronic configuration $\{\overline{P}_1, \overline{P}_2, \overline{P}_3, \ldots, \overline{P}_k, \ldots, \overline{P}_{k\,\max}\}$. The total energy of the ion for a given electronic configuration in AA is given in Rydberg units as

$$E_{\rm shm} = -\mathrm{Ryd} \sum_{k}^{k_{\max}} \overline{P}_k \frac{\overline{Z}_k^2}{n_k^2}, \tag{1}$$

where Ryd is the Rydberg constant and Z_k is the level screened charge given by

$$\overline{Z}_k = Z - \sum_{k'}^{k_{\max}} \sigma_{kk'} \left(1 - \frac{\delta_{kk'}}{D_k^0}\right) \overline{P}_{k'}, \tag{2}$$

where $\delta_{kk'}$ is the Kronecker delta, $\sigma_{kk'}$ is a set of screening constants that represent the interaction of an electron at level k with another electron at level k' in the multi electron system, $D_k^0 = 2(2l_k + 1)$ is the isolated atom degeneracy for the sub shell k, and $\overline{P}_k$ is the occupation number (average number of electrons in k) given by

$$\overline{P}_k = \frac{D_k}{1 + \exp\left[(\varepsilon_k + \Delta I - \mu)/kT\right]}, \tag{3}$$

where D_k is the density dependant degeneracy given by

$$D_k = \frac{D_k^0}{1 + \left[a_{zm}(r_k^0/R_{\rm ws})\right]^{b_{zm}}},$$

where a_{zm} and b_{zm} are the two empirical parameters. r_k^0 is the Bohr radius of the sub shell k

$$r_k^0 = a_0 \frac{3n^2 - l(l+1)}{2Z_k^0},$$

and $R_{\rm ws}$ is the Wigner–Seitz radius defined as

$$R_{\rm ws} = \left(\frac{4\pi\rho N_{\rm A}}{3A}\right)^{-1/3} = \left(\frac{4\pi n_i}{3}\right)^{-1/3},$$

where n_i is the ions number density, $N_{\rm A}$ the Avogadro number, and A is the mass number of the element. In Eq. (3), ΔI is the effective continuum lowering (CL) energy (which will be discussed below), μ is the chemical potential, kT is the thermal energy, and ε_k are the sub shell energies calculated as

$$\varepsilon_k = -\mathrm{Ryd}\,\frac{\overline{Z}_k^2}{n_k^2} + 2\,\mathrm{Ryd} \sum_{k'}^{k_{\max}} \overline{P}_{k'} \frac{\overline{Z}_{k'}^2}{n_{k'}^2} \sigma_{k'k} \left(1 - \frac{\delta_{kk'}}{D_k^0}\right). \tag{4}$$

The average charge state can be calculated by the charge neutrality condition as

$$\sum_{k}^{k_{\max}} \overline{P}_k + \overline{Z} = Z, \tag{5}$$

and chemical potential is adjusted by finding the root of the equation

$$\overline{Z} = \frac{4}{\sqrt{\pi}} \frac{A}{\rho N_A} \left(\frac{mkT}{2\pi\hbar^2} \right)^{3/2} f_{1/2}(\eta), \tag{6}$$

$f_{1/2}(\eta)$ is the Fermi–Dirac integral $f_\alpha(\eta)$, with $\alpha = 1/2$

$$f_\alpha(\eta) = \int_0^\infty \frac{x^\alpha}{1 + \mathrm{e}^{x-\eta}} \mathrm{d}x\,, \quad \eta = \frac{\mu}{kT}. \tag{7}$$

Equations (2)–(6) are solved self-consistently by using isolated atom data and initial guess for $\overline{Z}$ and η. The ion sphere model representation of CL as given in Ref. [18] is

$$\Delta I_{\mathrm{IS}} = c_{\mathrm{zm}}\, 3.6 \left(\frac{\overline{Z}}{R_{\mathrm{ws}}} \right), \tag{8}$$

where c_{zm} is a free parameter. The problem of this form is that the empirical parameter c_{zm} produces unrealistic average charge state results for values greater than or equal to 1 due to the double counting of degeneracy effects. In order to compensate for this discrepancy we have improved the continuum lowering energy calculations of Eq. (3) of SHML model by making it free from the empirical parameters and by adding exchange and correlation terms. We have bench-marked our results for average charge state calculation for different plasma conditions and studied the effect of this improved feature of I-SHML in Ref. [27], which is

$$\Delta I_{\mathrm{int}} = \frac{\bar{Z}}{R_{\mathrm{ws}}} \left[3.6 - 0.5 \frac{n_k^2}{Z_k^2 R_{\mathrm{ws}}^2} \left\{ n_k^2 - 3 l_k (l_k + 1) + 1 \right\} \right]. \tag{9}$$

This form is free from any empirical parameter and gives very close results with other standard codes. This form of CL is further improved with the addition of exchange and correlation effects. In SHML model, the central field approximation was assumed for many electron systems in which each particle moved in an independent effective hydrogenic potential. This approximation is not truly valid because the free electrons in AA cannot be treated as true free particles and must have some background interaction with other electrons. Therefore, we need to incorporate exchange and correlation effects especially for near and above solid densities. In I-SHML,[27] we only consider the local density approximation (LDA) for which, according to page 90 of Ref. [28], the exchange term derived by authors[29–31] is given by

$$E_{\mathrm{x}} = -0.916 \frac{\overline{Z}}{R_{\mathrm{ws}}} \text{ in unit (Ryd).} \tag{10}$$

The correlation effects are obtained from Padé approximal interpolation using plane wave approximation as

$$E_{\mathrm{c}} = 0.0621814 \left\{ \ln \frac{x^2}{x^2 + bx + c} + \frac{2b}{\sqrt{4c - b^2}} \arctan \frac{\sqrt{4c - b^2}}{2x + b} - \frac{bx_0}{x_0^2 + bx_0 + c} \left[\ln \frac{(x - x_0)^2}{x^2 + bx + c} + \frac{2(b + 2x_0)}{\sqrt{4c - b^2}} \arctan \frac{\sqrt{4c - b^2}}{2x + b} \right] \right\}, \tag{11}$$

where $b = 3.72744$, $c = 12.9352$, $x_0 = -0.10498$, and $x = \sqrt{R_{\mathrm{ws}}}$. Now the effective continuum lowering which is used in I-SHML becomes

$$\Delta I = \Delta I_{\mathrm{int}} + E_{\mathrm{x}} + E_{\mathrm{c}}. \tag{12}$$

With this form of effective continuum lowering, the energy levels ε_k are much more refined and give appreciable results for $\overline{Z}$ as bench-marked in our previous work.[27] Now we use this version to include the IPF calculations that are discussed in the next section.

3. Ion population fraction calculations in I-SHML

The simultaneous presence of different ions in plasma cannot be modeled directly within the AA approximation. In order to model IPF in hot dense plasma using the AA model, one starts with the quantum statistical representation of GPF which is written in terms of energy levels of the particles within GFP. The energy levels further require the information of number of particles, their population level, and the corresponding charge. Formally, the ion population fractions were calculated by using isolated atom data of energies in Saha–Boltzman equation, with CL taken into account along with some empirical cut off for the partition function. The problem with Saha–Boltzman equation is that it breaks down at higher ion densities.[32] Moreover, Saha–Boltzman is limited for non degenerate electrons at high temperature and low to moderate densities. The inclusion of different configurations interactions has been added which improves the results but does not solve the problem of the breakdown for higher densities. Another approximate solution is the use of binomial distribution for ion population fraction, which is based on the ideal Fermi Dirac gas model, e.g, used in NIMP model (non LTE ionized material package).[33] But that itself is based on the fact that

there is no correlation between electron probabilities which are dominant at higher densities and at low temperature. The result for binomial distribution and Saha Boltzman distribution matches for the low density and very high temperatures, but fails to predict the average charge state and IPF results at lower temperatures and at higher densities where strong interactions between electrons are dominant. Moreover, isolated energies are used under the approximation that the kinetic temperature is comparable to the isolated energies, which is questionable to date.[25,26] For the development of IPF in I-SHML, we follow the work of Ref. [25] for the development of the systematic integer charge state distribution around the average charge state using classical theory of fluctuations. The detailed derivation and discursion of these equations can be found in Ref. [25] as well as Refs. [34] and [35]. According to Ref. [25], the GPF for $Z+1$ ion system can be factorized and is given by

$$\mathscr{Z} = \sum_{Z'=0}^{Z} \left(\sqrt{\frac{(2\pi)^{k_{\max}}}{\det(\omega)}} \frac{\exp[-(1/2)\,(\Delta Z'/\sigma_{Z'})^2]}{\sqrt{2\pi}\sigma_{Z'}} \right), \tag{13}$$

where $\Delta Z' = \overline{Z} - Z'$ is the deviation of ionization state Z' from average charge state $\overline{Z}$ with the ion charge limitation $0 \le Z' \le Z$. $\sigma_{Z'}^2$ is the ionization variance around the average charge state and is defined as

$$\sigma_{Z'}^2 = \sum_{k,k'}^{k_{\max}} C_{k,k'}, \tag{14}$$

where $C_{k,k'}$ is the correlation matrix computed from the average atom values as

$$C_{k,k'} = (\omega)_{kk'}^{-1} = \overline{\Delta P_k \Delta P_{k'}}, \tag{15}$$

where $\Delta P_k = P_k^{Z'} - \overline{P_k}$ is the deviation of occupation number of level k of ionization state Z' from average atom occupation number $\overline{P_k}$. $P_k^{Z'}$ represents the occupation number of the k-th level in Z' ion, while $\omega_{kk'}$ is symmetric, definite, and positive matrix constructed from the electron–electron interaction energy matrix $V_{kk'}$ using average atom values for D_k and $\bar{P}_k$ as

$$\omega_{kk'} = \beta V_{kk'} + \frac{\delta_{kk'}}{\overline{\omega}_k^2}, \tag{16}$$

where $\beta = 1/k_{\mathrm{B}}T$ is the inverse of the thermal temperature which is in unit eV, and $V_{kk'}$ is the interaction energy of electron in level k with the electron in the level k' given as

$$V_{kk'} = \frac{\partial^2 E_{\mathrm{shm}}}{\partial \overline{P}_k \partial \overline{P}_{k'}}, \tag{17}$$

where E_{shm} is the total energy of the average atom given by Eq. (1) and

$$\overline{\omega}_k^2 = \frac{\bar{P}_k\,(D_k - \bar{P}_k)}{D_k}. \tag{18}$$

It is clearly seen from Eqs. (15), (16), and (18) that at higher temperatures, β tends to be zero and consequently

$$C_{k,k'} \approx \delta_{kk'}\,\overline{\omega}_k^2,$$

the correlation effects become negligible and we have non-interacting gas which is Fermi Dirac gas, and from Eq. (14) $\sigma_{Z'}^2$ approaches binomial distribution value $\sum_{k}^{k_{\max}} \overline{\omega}_k^2$. On the other hand, at lower temperatures, correlation effects dominate and we have an interacting electron distribution given by electron–electron interaction energy matrix $V_{kk'}$

$$C_{k,k'} \approx k_{\mathrm{B}}T\,(V^{-1})_{kk'}.$$

In this way $\sigma_{Z'}^2$ will give us the signatures for interaction effects over a wide range of densities and temperatures for the calculation of IPF. Once $\sigma_{Z'}^2$ is calculated using AA I-SHML, the normalized IPF can be calculated using $\sigma_{Z'}^2$ as

$$\mathscr{F}_{\mathscr{Z}'} = \frac{\exp(-1/2)\,(\Delta Z'/\sigma_{Z'})^2}{\sum_{Z'=0}^{Z} \exp[-(1/2)\,(\Delta Z'/\sigma_{Z'})^2]}. \tag{19}$$

The above equation gives a fast calculation of IPF and it inherently includes the interaction energy between different electrons through $V_{kk'}$ and exchange and correlation effects in $\overline{Z}$. In this way, the IPF results obtained from the above equations are better than SHML, and are comparable with other standard codes over a wide range of densities and temperatures.

4. Results and discussion

We have implemented the IPF calculations using Eqs. (13)–(19) in our I-SHML model. To check the correctness of our implementation, we first compare our model with SHML for IPF for aluminum plasma in Fig. 1(a) and average charge state in Fig. 1(b). The difference in the results is due to the inclusion of improved CL with exchange and correlation effects. A detailed discussion on this point can be found in our previous work.[27] For more elaboration of this point, we have compared in Fig. 2 the ionization variance σ_Z and in Fig. 3 the corresponding average charge state of the two models for a wide range of temperaturse (from 1 eV to 1 keV) at different mass densities of aluminum plasma. It is obvious from Fig. 2 that there is no difference between the two models at low mass densities and noticeable difference at higher mass densities. This is due to the fact that at higher densities, the effect of exchange and correlation in the calculation of CL is higher compared to that at lower densities. In SHML model, all bound levels are shifted by the same amount of CL, which causes unrealistic results of the average charge state. This point is also discussed in detail in our previous work.[27] We see that σ_Z in Fig. 2 at 1 g/cc varies abruptly for SHML results. This is due to the fact that the ionization variance is the measure of fluctuation of ionization, i.e., if ionization varies

abruptly, so does the σ_Z. At low temperatures and near solid density where plasma is degenerate, the SHML model gives an unrealistic charge state. As can be seen clearly from Fig. 3, the average charge state by SHML abruptly changes between 2 eV and 5 eV at 1 g/cc because of the inappropriate choice of CL as mentioned in this manuscript as well as in our previous results.[27] At 10 g/cc the result of average charge state changes smoothly over the entire range of temperatures, and consequently σ_Z changes smoothly. Compared to SHML, our I-SHML model with proper choice of CL gives smooth and consistent results of average charge state for the cases of 1 g/cc and 10 g/cc.

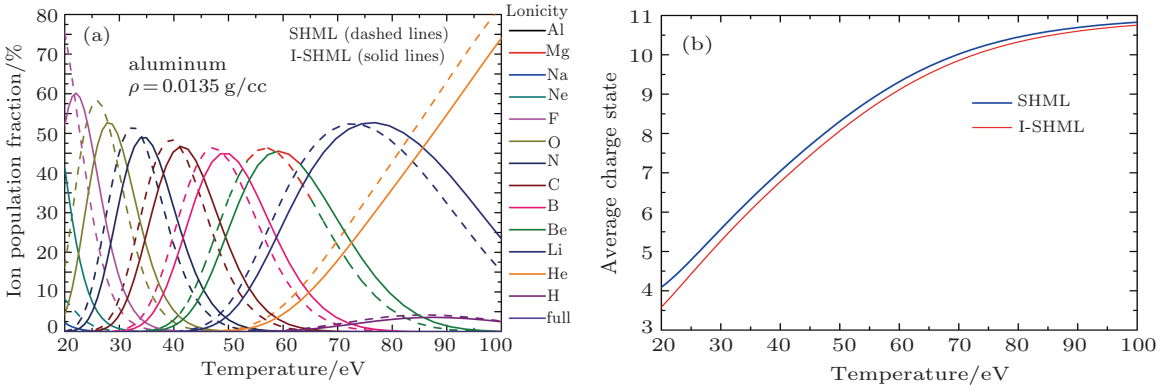


Fig. 1. (color online) (a) Comparison of ion population percent fraction between I-SHML and SHML for aluminum plasma at a density of 0.0135 g/cc as a function of temperature. (b) Comparison of average charge state between I-SHML and SHML models for aluminum plasma at a density of 0.0135 g/cc as a function of temperature.

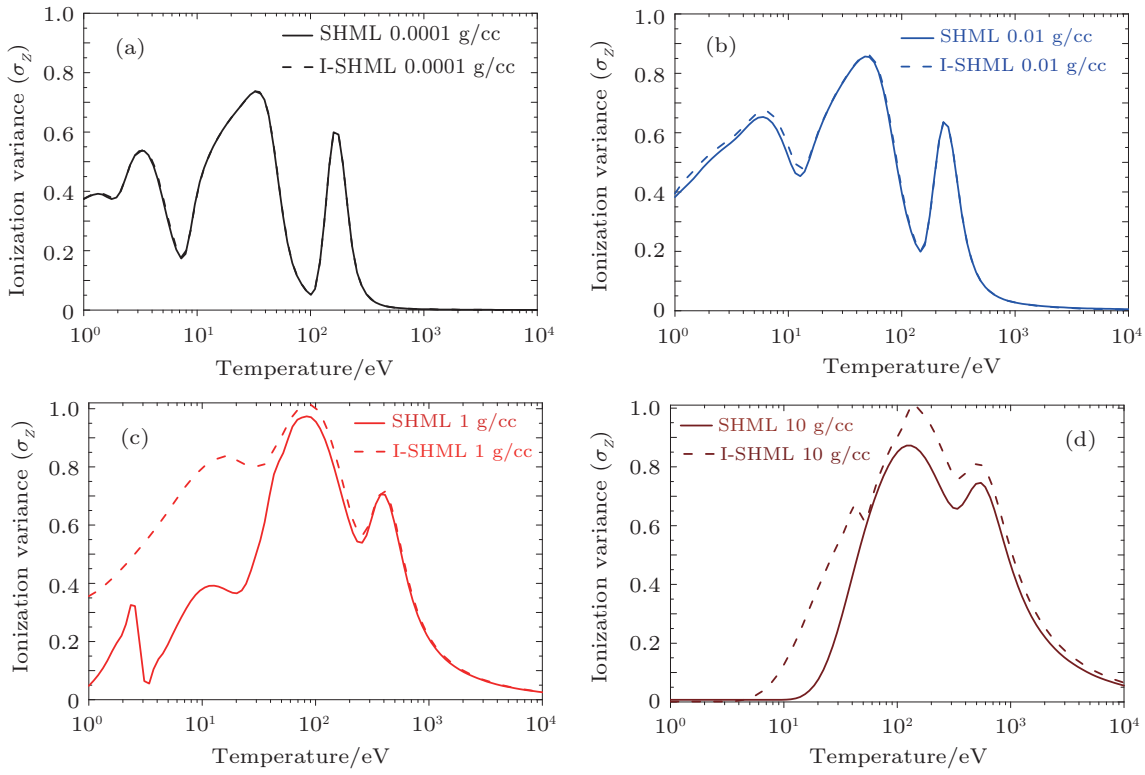


Fig. 2. (color online) Comparison of ionization variance between SHML model and I-SHML model for aluminum plasma at a temperature range of 1 eV to 10 keV and at densities of 0.0001 g/cc (a), 0.01 g/cc (b), 1.0 g/cc (c), and 10.0 g/cc (d).

We have compared the results of our model with several other models as well. The most important is the model of the Kiyokawa[17] that uses a multi average ion (Multi-AIM) formulism developed for hot dense plasma. Multi-AIM uses finite temperature density functional theory (FTDFT), in which pair correlation functions are obtained self consistently by minimizing the free energy of the system. They have also included the exchange and correlation potentials in their calculations, and self consistency for IPF is achieved using Saha equation. We have compared our results of IPF for low density (0.0081 g/cc) iron plasma at different temperatures with Multi-AIM model in Fig. 4. Very good agreement at a low temperature of 25 eV is found with the increase of the temperature. We have found a slight change of the IPF peak position and the profile shape. The I-SHML model is showing a better structural profile due to the exchange and correlation potential in this model. The data for the comparison is taken from the tables provided in the reference.

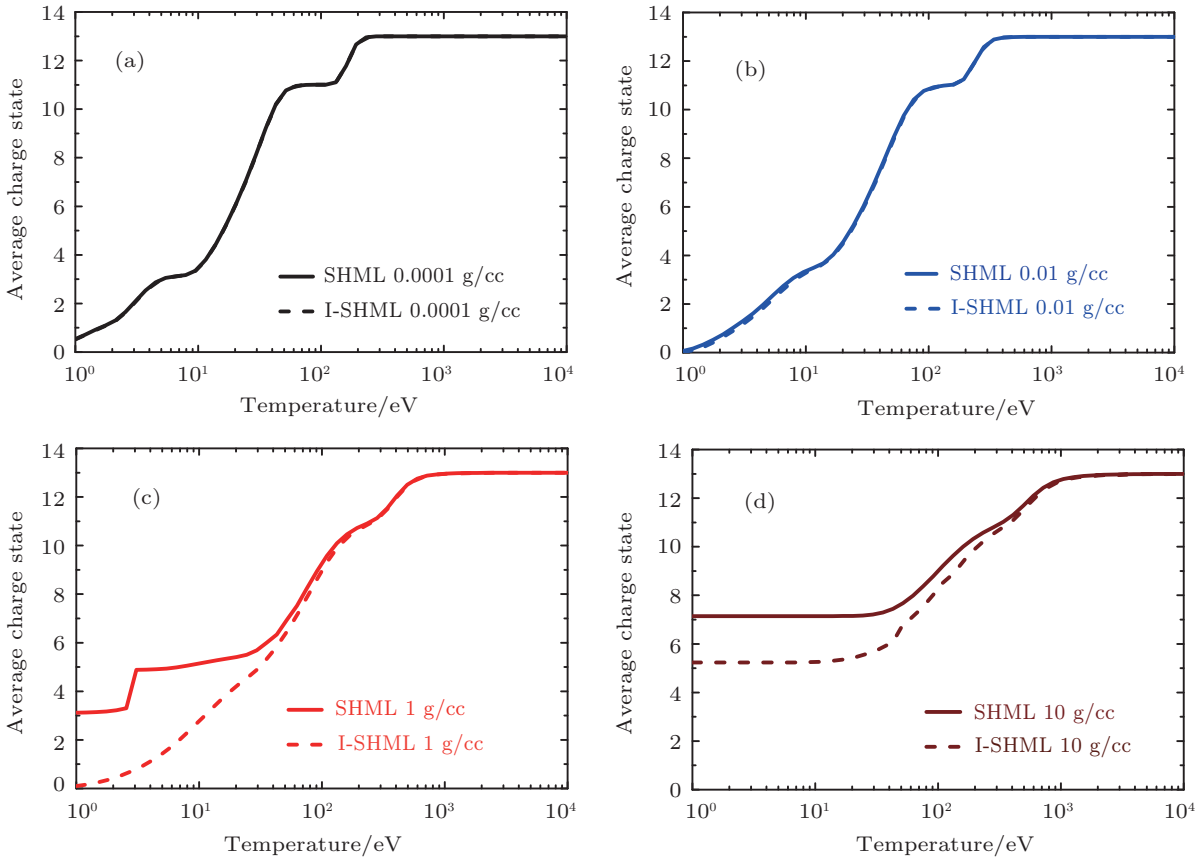


Fig. 3. (color online) Comparison of $\overline{Z}$ for aluminum between SHML and I-SHML models at a temperature range of 1 eV to 10 keV and at densities of 0.0001 g/cc (a), 0.01 g/cc (b), 1.0 g/cc (c), and 10.0 g/cc (d).

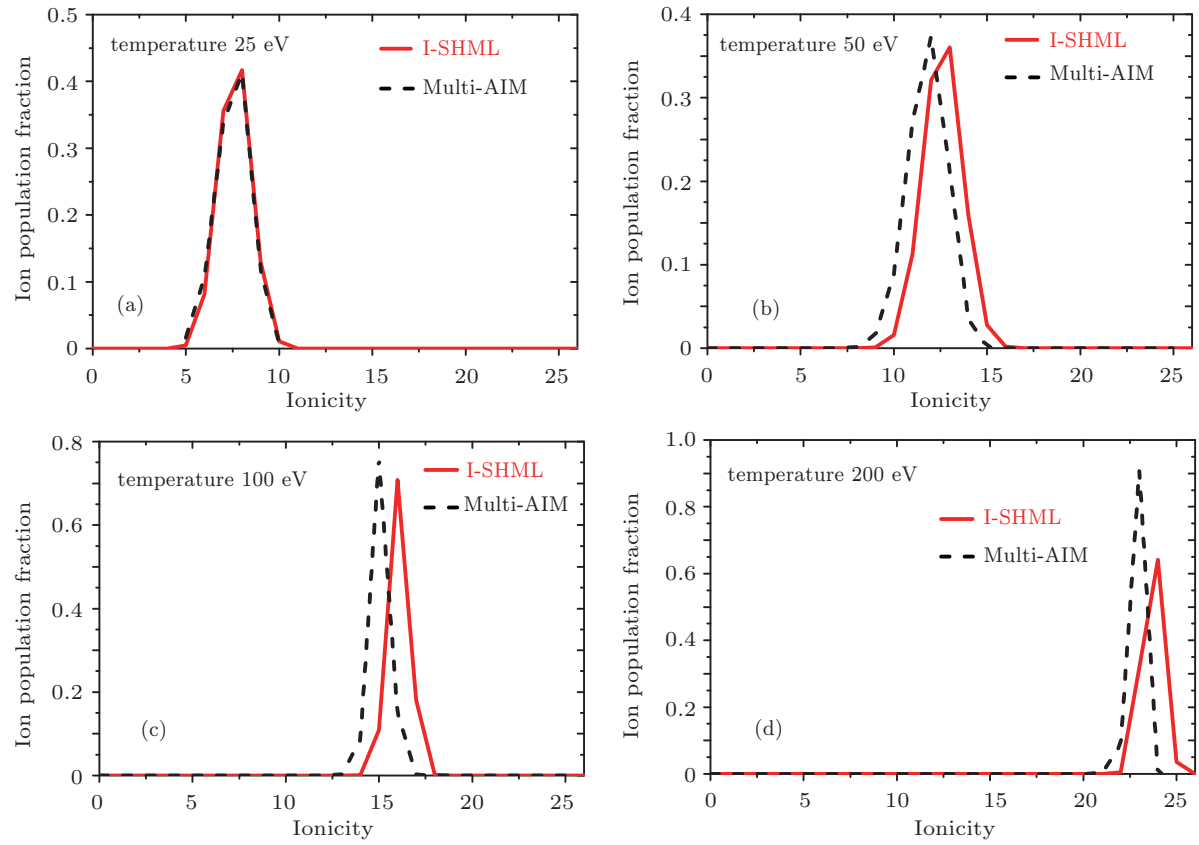


Fig. 4. (color online) Comparison of charge state distribution of Fe plasma at an ion density of 0.0081 g/cc and temperatures of 25 eV (a), 50 eV (b), 100 eV (c), and 300 eV (d), respectively, between Multi-AIM and I-SHML model.

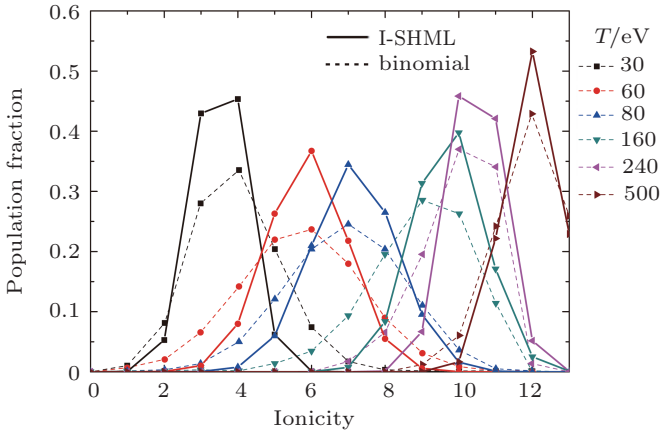


Fig. 5. (color online) Comparison of IPF of I-SHML (solid lines) with binomial distribution model (dased lines) for aluminum at a solid density of 2.7 g/cc and at temperatures 30 eV, 60 eV, 80 eV, 160 eV, 240 eV, and 500 eV.

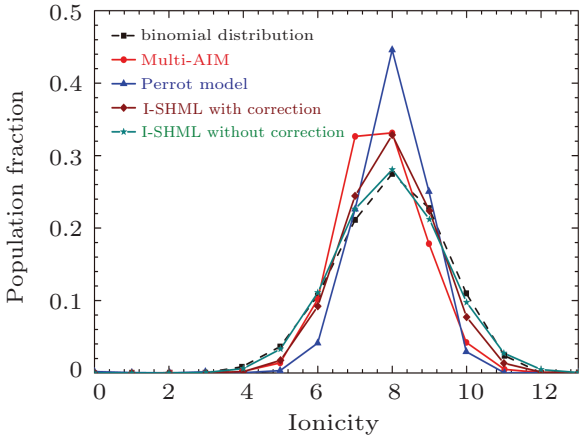


Fig. 6. (color online) Ion population fractional of average ions in an Al plasma at an ion density of 2.77 g/cc and a temperature of 100 eV, where the red line indicates that obtained by Multi-AIM, the blue line indicates Perrot's result,[37] and the black line is for the binomial distribution. The I-SHML results are drawn by the wine color and sea green lines that stand for the cases with and without correlation, respectively.

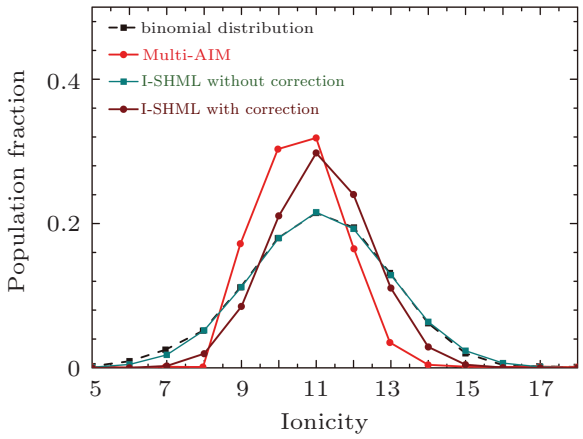


Fig. 7. (color online) Comparison of the charge state distribution of Fe plasma at an ion density of 7.874 g/cc and a temperature of 100 eV, among the binomial model, Multi-AIM, and I-SHML results with and without correlation.

In Fig. 5, we have compared the IPF calculations of solid density aluminum plasma with the binomial distribution model by Son *et al.*[36] at temperatures of 30 eV to 500 eV . This model uses a two step method for the construction of IPF. In the first step it performs the average atom calculations using self consistent Hatree–Fock method, and in the next step it computes the IPF using binomial distribution formula by selecting a limited number of possible excited configurations. They also presented the effect of CL energy on the average charge state using average atom model. The peaks in the binomial model have lower values for all temperatures, which is due to the fact that this model is ideal for Fermi Dirac gas and underestimates the IPF predictions. For elaboration of this point, we have compared our IPF calculations with and without correlation effects for solid density aluminum plasma and iron plasma in Figs. 6 and 7, respectively, among different models.

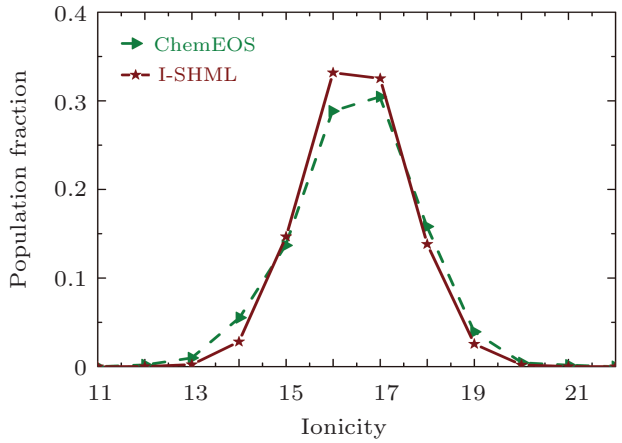


Fig. 8. (color online) Comparison of IPF of I-SHML with the ChemEOS code for iron at an ion density of 10^{23} and at a temperature of 192.91 eV.

The comparison of I-SHML calculations with ChemEOS model is presented in Fig. 8 for iron plasma. We found very close agreement between the two models, as the ChemEOS model is based on the interacting particle theory that uses Plank–Larkin partition function with particles interaction taken into account. This shows the validity of our I-SHML model. In Fig. 9, we have compared IPF calculation for aluminum plasma at 400 eV temperature and at different densities with detail level calculations by Li *et al.*[38] The results are in excellent agreement because of the high temperature. This shows that I-SHML model gives very reasonable results for hot dense plasma in comparison with detailed level calculation. We also compared the results with Zeng *et al.*[39] who used detailed term accounting approximation for the calculation of IPF for aluminum plasma at 20 eV and a low density of 0.01 g/cc. The average charge state is the same but profiles deviate because Jiaolong calculation relay on the Saha ionization model and they have used a large number of configurations for their calculation. Also they have used Debye–Huckel model for CL model which is also the cause of the deviation.

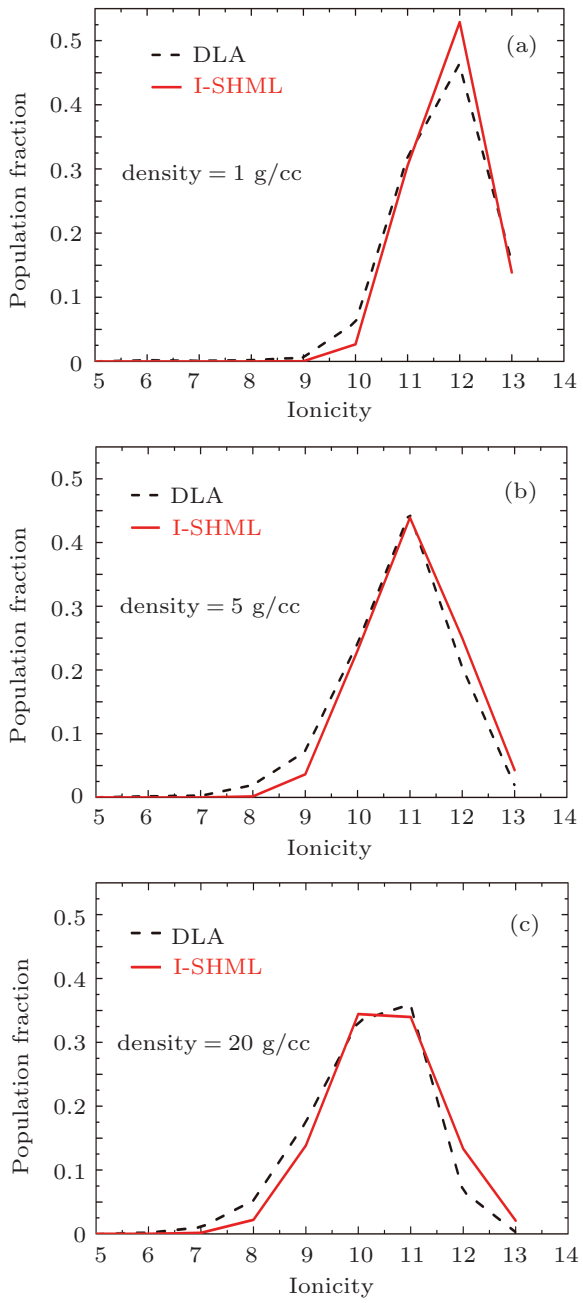


Fig. 9. (color online) Comparison with detail level calculation of Ref. [38] for aluminum plasma at a temperature of 400 eV and at different densities of 1 g/cc (a), 5 g/cc (b), and 20 g/cc (c).

5. Summary and conclusion

The IPF calculations for the hot dense matter are very important to understand the emitted complex radiative spectra from the experiments which show the presence of different ions with composite electronic structures. These multiplex electronic structures in dense plasmas are due to CL phenomenon which arises due to the interaction between bound and free electrons. The calculation of IPF involves the solution of GPF for interacting electrons, which is obtained either from DL calculations or by the AA model using classical theory of fluctuations. In this study, we present the IPF calculations under the LTE plasma conditions based on classical theory of fluctuations using I-SHML which contains the improved form of CL. The results of IPF computations for aluminum and iron are compared with the published literature of Saha model and binomial distribution models, and are correspondingly discussed. Good agreement is found for high temperature and low density plasma conditions with binomial and Saha models. Some deviations are seen for low temperature and high density plasma conditions where there are strong correlation interactions which are not addressed in binomial and Saha models. Our results gives good estimate for IPF over a wide range of densities and temperatures due to the presence of CL and correlation effects.

References

[1] Bell A R, Davies J R, Guerin S and Ruhl H 1997 *Plasma Phys. Control. Fusion* **39** 653
[2] Hoffmann D H H, Blazevic A, Ni P, Rosmej O, Tauschwitz A, Udrea S, Varentsov D, Weyrich K and Maron Y 2005 *Laser Part. Beams* **23** 47
[3] Larsen J and Colvin J 2014 *Properties and Behavior of Matter At Extreme Conditions* (Cambridge: Cambridge Univ. Press)
[4] Zeng J, Gao C and Yuan J 2010 *Phys. Rev. E* **82** 026409
[5] Zeng J, Yuan J and Lu Q 2001 *Phys. Rev. E* **64** 066412
[6] Rose S J, van Hoof P A M, Jonauskas V, Keenan F P, Kisielius R, Ramsbottom C, Foord M E, Heeter R F and Springer P T 2004 *J. Phys. B: At. Mol. Opt. Phys.* **37** L337
[7] Wang F, Fujioka S, Nishimura H, Kato D, Li Y, Zhao Gang, Zhang Jie and Takabe H 2008 *Phys. Plasmas* **15** 073108
[8] Wang F, Han B, Jin R, Salzmann D, Liang G, Wei H, Zhong J, Zhao G and Li J 2016 *J. Phys. B: At. Mol. Opt. Phys.* **49** 064013
[9] Rogers F J and Iglesias C A 1995 *Highlights Astron.* **10** 573
[10] Kilcrease D P, Colgan J, Hakel P, Fontes C J and Sherrill M E 2015 *High Energy Density Phys.* **16** 36
[11] Hakel P, Sherrill M E, Mazevet S, Abdallah Jr, Colgan J, Kilcrease D P, Magee N H, Fontes C J and Zhang H L 2006 *J. Quantum Spectrosc. Radiat. Transfer* **99** 265
[12] Nikiforov A F, Novikov V G and Uvarov V B 2005 *Quantum-Statistical Models of Hot Dense Matter: Methods for Computation Opacity and Equation of State* (Basel: Birkhäuser Verlag) ISBN: 978-3-7643-7346-7
[13] Crowley B J B and Harris J W 2001 *J. Quantum Spectrosc. Radiat. Transfer* **71** 257
[14] Kouser R, Tasneem G, Shahzad M S, Sardar S, Ali A, Nasim M H and Salahuddin M 2017 *Chin. Phys. B* **26** 075201
[15] Faussurier G 2000 *J. Quantum Spectrosc. Radiat. Transfer* **65** 207
[16] Blenski T, Piron R, Caizergues C and Cichocki B 2013 *High Energy Density Phys.* **9** 687
[17] Kiyokawa S 2014 *High Energy Density Phys.* **13** 40
[18] Faussurier G, Blancard C and Decoster A 1997 *J. Quantum Spectrosc. Radiat. Transfer* **58** 223
[19] Faussurier G, Blancard C and Renaudin P 2008 *High Energy Density Phys.* **4** 114
[20] Mendoza M A, Rubiano J G, Gil J M, Rodriguez R, Florido R, Martel P and Minguez E 2012 *39th EPS Conference on Plasma Physics* 2012, *EPS* 2012 *and the 16th International Congress on Plasma Physics*, July 2–6, 2012, Stockholm, Sweden, ISBN: 2-914771-79-7, p. 5.167
[21] Blancard C and Faussurier G 2003 *J. Quantum Spectrosc. Radiat. Transfer* **81** 65
[22] Green J M 1964 *J. Quantum Spectrosc. Radiat. Transfer* **4** 639
[23] Perrot F 1988 *Physica A* **150** 357
[24] Wilson B G 1993 *J. Quantum Spectrosc. Radiat. Transfer* **49** 241
[25] Faussurier G, Blancard C and Decoster A 1997 *Phys. Rev. E* **56** 3474
[26] Faussurier G, Blancard C and Decoster A 1997 *Phys. Rev. E* **56** 3488
[27] Ali A, Shabbir Naz G, Shahzad M S, Kouser R, Rehman A and Nasim M H 2018 *High Energy Density Phys.* **26** 48

[28] Huebner W F and Barfield W D 2014 *Opacity* (New York: Springer-Verlag)
[29] Seitz F 1940 *The Modern Theory of Solids* (New York: McGraw-Hill)
[30] Kittel C 1936 *Quantum Theoy of Solids* (New York: John Wiley and Sons)
[31] Cowan R D 1981 *The Theory of Atomic Structure and Spectra* (Berkeley, Los Angeles, London: University of California Press)
[32] Sweeney M A 1978 *Astrophys. J.* **220** 335
[33] Rose S J 1997 *The NIMP (Non-LTE Ionised Material Package) Code*, Rutherford Appleton Laboratory, RAL-TR–97-020, United Kingdom
[34] Negele J H and Orland H 1988 *Quantum Many Particle Systems* (New York: Addison Wesley)
[35] Feynmen R P 1972 *Statitical Mechanics: A Set of Lectures* (New York: Addison Wesley), ISBN: 0805325085, 0805325093
[36] Son S K, Thiele R, Jurek Z, Ziaja B and Santra R 2014 *Phys. Rev. X* **4** 031004
[37] Perrot F 1987 *Phys. Rev. A* **35** 1235
[38] Li Y, Wu J, Houv Y and Yuan J 2009 *J. Phys. B: At. Mol. Opt. Phys.* **42** 235701
[39] Zeng J, Yuan J and Lu Q 2001 *Phys. Rev. E* **64** 066412